DOI 10.1007/s11182-020-01921-y

Russian Physics Journal, Vol. 62, No. 10, February, 2020 (Russian Original No. 10, October, 2019)

OPTICS AND SPECTROSCOPY

INVESTIGATION OF ABSORPTION AND EMISSION SPECTRA OF NITROGEN OXIDES NO, N_2O, NO_2, AND N_2O_4

N. I. Moskalenko, O. R. Kluchnikov, S. N. Parzhin, and I. R. Dodov UDC 629.125:551.521

The absorption and emission spectra of NO, N_2O, NO_2, *and* N_2O_4 *nitrogen oxides have been studied with high and intermediate spectral resolution in the range 0.25–25 μm under conditions of self-broadening and nitrogen-induced broadening at room and enhanced temperatures. The experimental data on the spectral transmittance function have been parameterized by the two-parameter equivalent mass method. The rovibrational band intensities have been measured and the data on the absorption induced by the pressure in collisions of* NO_2–NO_2 *molecules have been obtained.*

Keywords: nitrogen oxides, spectral transmittance function, pressure-induced absorption, rovibrational spectra, radiative transfer.

INTRODUCTION

A solution of many applied problems of radiative transfer in the atmosphere of our planet and of heat exchange in power engineering installations as well as of anthropogenic impact on weather and climate of the Earth [1–9] requires data on the optical characteristics of gaseous components. Nitrogen oxides NO, N_2O, NO_2, and N_2O_4 are present in the Earth atmosphere, emissions of active volcanoes, heat technology media of power engineering and energy technology installations, and aircraft and automobile engines. In [2, 4–6], a high efficiency of application of fine structure spectrometry is shown for the determination of ingredients of combustion products of fires, burning wood, combustion chambers of electric power units, and emissions in the atmosphere of combustion products of automobile and aircraft engines. Nitrogen oxides strongly absorb not only in the IR spectral range, but also in the UV and visible spectral ranges. The data on the radiative characteristics of nitrogen oxides are also required for modeling of the emission spectra of natural background components of the Earth and the atmosphere, zonal modeling of radiative heat exchange, and forecasting of anthropogenic climate changes [5, 6, 8, 9]. In the present work, results of experimental investigations of the radiative characteristics of nitrogen oxides using spectral measuring complexes of different functional designations [1, 2, 10–12] are considered.

HIGH-RESOLUTION SPECTROMETRY OF NITROGEN OXIDES

The main objective of experimental investigations of the absorption spectra of nitrogen oxides with high spectral resolution is to obtain data necessary for an analysis of ingredients of nitrogen oxides in products of combustion of energetic fuels and in anthropogenic atmospheric emissions by the method of fine structure spectrometry. Experimental investigations were carried out in the UV, visible, and IR spectral ranges. It is important to

Kazan State Power Engineering University, Kazan, Russia, e-mail: NikMoskalenko@list.ru; olegkgeu@ya.ru; Parjin@yandex.ru; utisey@gmail.com. Translated from Izvestiya Vysshikh Uchebnykh Zavedenii, Fizika, No. 10, pp. 137–147, October, 2019. Original article submitted February 13, 2018; revision submitted July 3, 2019.

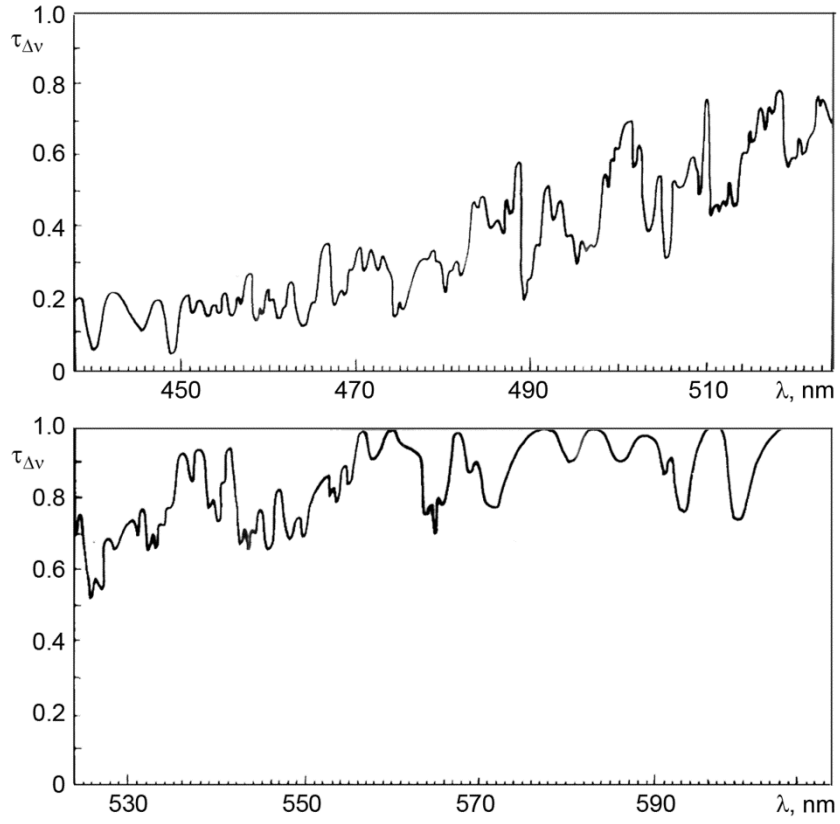

Fig. 1. Experimental absorption spectrum of nitrogen dioxide at 0.45–0.6 μm for the NO_2 content $W_{NO_2} = 0.25$ atm·cm, the pressure $P_{NO_2} = 0.025$ atm, and $T = 300$ K.

note that the fine structure of spectra of nitrogen oxides allows the contribution of NO_2 and N_2O_4 molecules to the recorded together with the pressure-induced absorption (PIA) caused by the quadrupole moment induced in collisions of NO_2–NO_2 molecules. Experimental investigations were carried out using high spectral resolution measuring complexes described in [1, 2, 10–12]. Figure 1 shows an example of the NO_2 absorption spectrum measured in the visible range at 440–600 nm at a temperature of 300 K. The short-wavelength wing of the electronic NO_2 spectrum is stretched up to 250 nm. Note that the NO_2 emission in flames is nonequilibrium [1, 2]. At high vibrational temperatures, the NO_2 emission spectrum broadened toward red region up to 800 nm.

Figure 2 shows an example of the measured rovibrational (RV) NO_2 absorption spectrum at 2860–2940 cm^{-1}. Unlike NO_2, the fine structure of the spectrum of N_2O_4 molecules is practically not pronounced because of dense packing of the absorption spectral lines (ASL), and in the pressure-induced NO_2 absorption bands, the fine structure of the spectrum is completely smeared.

The NO ASL parameters were measured at temperatures in the interval 300–900 K. The NO molecule is in a non-singlet electronic state. The ground NO state is $^2\Pi$ which is split during spin-orbit interaction into $^2\Pi_{1/2}$ and $^2\Pi_{3/2}$ components corresponding to anti-parallel and parallel orbital moments and spin projections. In addition to the $^2\Pi_{3/2}$–$^2\Pi_{3/2}$ and $^2\Pi_{1/2}$–$^2\Pi_{1/2}$ ASL components in the NO spectrum, weak $^2\Pi_{3/2} \leftrightarrow {}^2\Pi_{1/2}$ bands-satellites can be present in the spectrum, whose intensities are approximately by four orders of magnitude weaker than the intensity of the fundamental bands. It is convenient to consider the energy of the NO molecule as the energy of two simple diatomic molecules whose electronic levels are separated by $Q_v = 123.209$ cm^{-1}. Each NO band has *R*-, *Q*-, and *P*-branches. In addition, ℓ-doubling takes place for the NO bands. In [13] the high-temperature atlas of the NO ASL parameters is tabulated for the fundamental and overtone bands at the temperature $T_0 = 900$ K. Figure 3 shows an example of its application for calculation of the spectral absorption coefficient of the fundamental NO band at temperatures $T \in \{300, 3000\}$ K. The

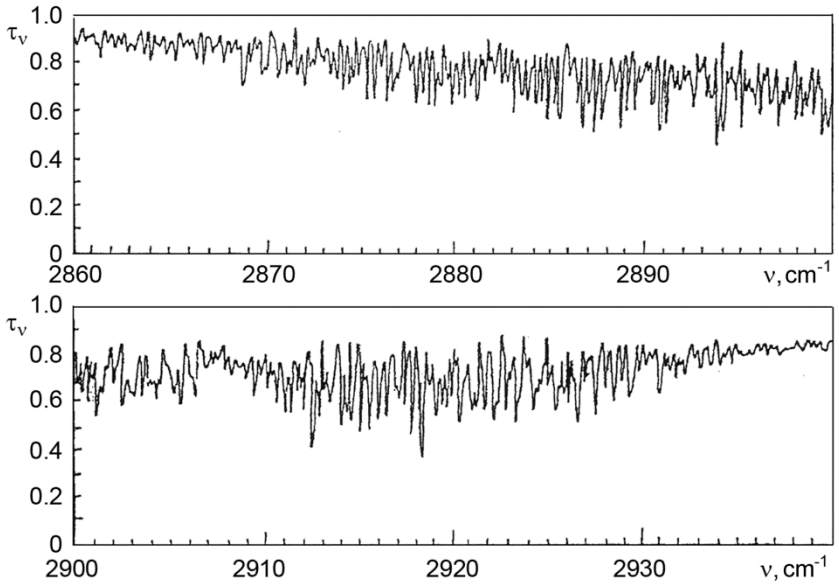

Fig. 2. NO_2 absorption spectrum at 2860–2940 cm^{-1} with the resolution $\Delta = 0.107$ cm^{-1} at the pressure $P_{NO_2} = 0.063$ atm, the NO_2 content $w = 0.63$ atm·cm, and the temperature $T = 293$ K.

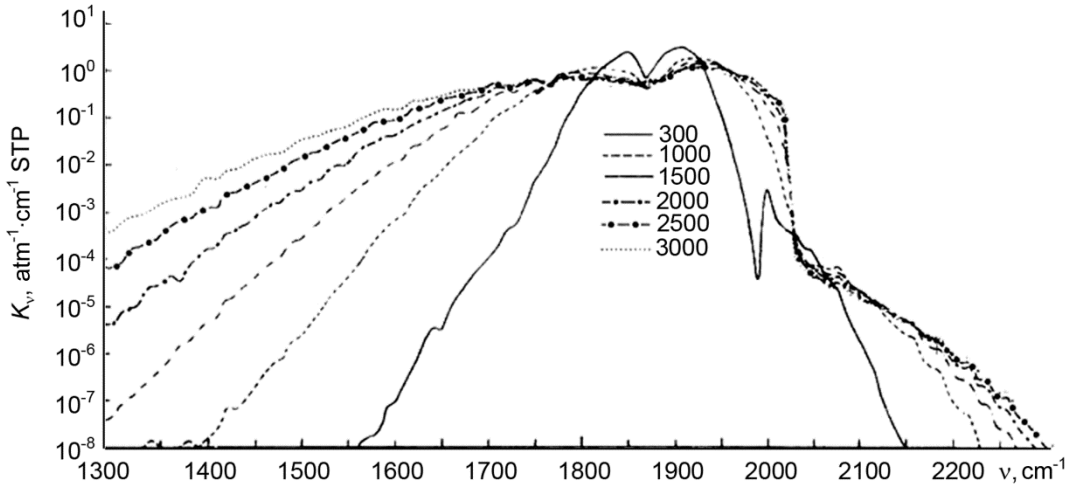

Fig. 3. Absorption coefficients in the NO fundamental bands around 4.54 μm at temperatures in the interval 300–3000 K.

integral intensity of the fundamental NO band was $S_{int} = 122$ $atm^{-1}·cm^{-2}$ STP. When preparing the atlas of the ASL parameters, transitions with vibrational and rotational quantum numbers $V \in \{0; 10\}$ and $J \in \{0.5; 119.5\}$ were taken into account. The ASL intensity was described by the rigid top model for $^{14}N^{16}O$, $^{15}N^{16}O$, $^{14}N^{18}O$, and $^{15}N^{18}O$ isotope bands. The dependence of the ASL halfwidth $\alpha(J)$ was chosen according to the data of experimental investigations. The NO ASL intensity and halfwidth were recalculated for other temperatures using the well-known spectroscopic relationships

$$S_i(T) = S_i(T_0)\frac{Q(T_0)}{Q(T)}\frac{1-\exp\left(-\frac{\nu_i k}{T}\right)}{1-\exp\left(-\frac{\nu_i k}{T_0}\right)}\exp\left[-E_i k\left(\frac{1}{T}-\frac{1}{T_0}\right)\right], \quad (1)$$

$$\alpha_i(T) = \alpha_i(T_0)\left(\frac{T_0}{T}\right)^n, \quad (2)$$

where $k = 1.439$, i is the line number, Q is the partition function, and n is empirical parameter. The possibility of description of the ASL intensities at temperatures in the interval 220–900 K by the rigid top model was experimentally confirmed in [1, 2, 5].

The nitrous oxide (N_2O) spectra with high spectral resolution were measured in the vicinity of the 00^00–121 (4630.31 cm^{-1}), 00^00–02^02 (4417.51 cm^{-1}), 00^00–10^01 (3481.2 cm^{-1}), 02^01 (3365.6 cm^{-1}), 00^00–20^00 (2563.5 cm^{-1}), 00^00–12^00 (2461.5 cm^{-1}), 00^00–00^01 (2223.5 cm^{-1}), and 00^00–01^10 (588.8 cm^{-1}) RV bands. The spectral resolution $\Delta = 0.06$–0.15 cm^{-1} depended on the investigated spectral range [14]. The ASL intensities and halfwidths were determined by the method of differential moments of decomposition of the spectrum with optical thickness $|\ln\tau_\nu|$ into separate lines and spline approximation of the recorded spectrum by a fifth degree polynomial to exclude noise with subsequent allowance for the influence of the instrumental function [5, 7]. As an example, Table 1 presents experimental data on the ASL intensities and halfwidths in the ν_3 band of the N_2O molecule, where $\overline{S}_R$ and $\overline{S}_P$ are the ASL intensities for the *R*- and *P*-branches; α_{RN_2O} and α_{RN_2O} are the ASL halfwidths for the *R*- and *P*-branches and nitrogen (N_2) broadening and self-broadening; ν_R and ν_P are the ASL centers for the *R*- and *P*-branches; and $J_{R,P}$ are the rotational quantum numbers of transitions for *R*- and *P*-branches.

The intensity $S(J)$ of the N_2O line, where J is the rotational quantum number, is given by the relationships

$$S(J) = \frac{\nu}{\nu_0}F(J'')\frac{S_\nu S_R}{Q_\nu Q_R}, \quad (3)$$

$$S_R = gL\exp\left[\frac{-kE^*_\nu}{T}\right], \quad (4)$$

$$Q_R = \sum_{J''} g_{J''}(2J''+1)\exp\left[\frac{-kE''_R}{T}\right], \quad (5)$$

$$E_R = B''J''(J''+1) - D''\left[J''(J''+1)\right]^2, \quad (6)$$

where S_ν is the vibrational factor determining the RV band intensities, S_R is the force of the rotational transition line, ν is the ASL position, ν_0 is the position of the center of the RV band, g is the amplitude multiplier, E''_R is the rotational energy of the ground state, Q_ν is the vibrational partition function, Q_R is the rotational partition function, L is the amplitude factor, $F(J'')$ is the value of the *F*-factor, and $k = 1.439$. The ASL intensities $\overline{S}$ were also measured, and the dependences $\overline{S}(J)$ were obtained with an error no more than 10 %. The data obtained were used to determine the parameters of the *F*-factor given by the empirical relationship

$$F = 1 + a_1 m + a_2 m^2, \quad (7)$$

TABLE 1. Experimental Data on the Spectral Absorption Line Intensities and Halfwidths in the ν_3 Band of the N_2O Molecule at $T = 296$ K

$J_{R,P}$	ν_R, cm^{-1}	$\overline{S}_R$, $cm^{-2}\cdot atm^{-1}$	α_{RN_2}, $см^{-1}\cdot atm^{-1}$	α_{RN_2O}, $cm^{-1}\cdot atm^{-1}$	ν_P, cm^{-1}	$\overline{S}_P$, $cm^{-2}\cdot atm^{-1}$	α_{PN_2}, $cm^{-1}\cdot atm^{-1}$	α_{PN_2O}, $cm^{-1}\cdot atm^{-1}$
0	2224.587	2.66	0.083	0.107				
1	2225.412	5.99	0.081	0.104	2222.918	2.99	0.082	0.103
2	2226.229	8.90	0.080	0.101	2222.073	5.93	0.080	0.100
3	2227.039	11.73	0.079	0.098	2221.222	8.79	0.080	0.099
4	2227.843	14.43	0.078	0.096	2220.363	11.50	0.079	0.098
5	2228.639	17.02	0.078	0.094	2219.497	14.10	0.079	0.096
6	2229.438	19.30	0.077	0.094	2218.625	16.50	0.078	0.095
7	2230.216	21.50	0.076	0.092	2217.745	18.70	0.077	0.094
8	2230.987	23.40	0.075	0.091	2216.859	20.80	0.076	0.093
9	2231.756	25.10	0.075	0.090	2215.966	22.48	0.075	0.092
10	2232.518	26.50	0.075	0.088	2215.066	23.98	0.075	0.091
11	2233.273	27.64	0.074	0.088	2214.159	24.97	0.075	0.090
12	2234.021	28.50	0.074	0.086	2213.246	26.19	0.074	0.089
13	2234.762	29.20	0.073	0.084	2212.325	26.93	0.074	0.087
14	2235.496	29.60	0.072	0.083	2211.398	27.40	0.073	0.086
15	2236.223	29.80	0.071	0.083	2210.464	28.00	0.073	0.085
16	2236.943	29.20	0.070	0.082	2209.523	28.10	0.072	0.084
17	2237.656	29.10	0.069	0.080	2208.575	28.00	0.070	0.082
18	2238.362	28.60	0.068	0.079	2207.620	26.90	0.069	0.081
19	2239.062	28.00	0.067	0.077	2206.658	26.40	0.067	0.080
20	2239.754	27.20	0.066	0.075	2205.690	25.60	0.067	0.078
21	2240.439	26.10	0.065	0.074	2204.715	24.70	0.064	0.077
22	2241.117	25.30	0.064	0.073	2203.733	23.60	0.065	0.075
23	2241.788	24.10	0.064	0.073	2202.744	22.50	0.065	0.074
24	2242.453	22.70	0.064	0.073	2201.748	21.31	0.065	0.073
25	2243.110	21.20	0.063	0.072	2200.747	20.10	0.064	0.072
26	2243.760	19.80	0.063	0.071	2199.736	18.80	0.064	0.070
27	2244.403	18.00	0.063	0.070	2198.721	17.50	0.064	0.070
28	2245.039	17.00	0.063	0.070	2197.698	16.20	0.064	0.070
29	2245.668	15.64	0.063	0.069	2196.668	14.90	0.064	0.070
30	2246.291	14.33	0.063	0.069	2195.632	13.60	0.064	0.070
31	2246.906	13.50	0.063	0.068	2194.589	12.40	0.063	0.069
32	2247.514	12.1	0.063	0.068	2193.539	11.3	0.063	0.068
33	2248.115	10.7	0.063	0.068	2192.483	10.2	0.063	0.068
34	2248.709	9.57	0.063	0.067	2191.419	9.15	0.062	0.068
35	2249.296	8.45	0.063	0.067	2190.349	8.20	0.062	0.067
36	2249.876	7.60	0.063	0.067	2189.273	7.30	0.062	0.067
37	2250.449	6.73	0.063	0.067	2188.188	6.42	0.062	0.067
38	2251.015	5.93	0.063	0.065	2187.098	5.66	0.062	0.066
39	2251.573	5.22	0.063	0.065	2186.002	5.74	0.062	0.066
40	2252.125	4.53	0.062	0.065	2184.898	4.33	0.062	0.066
41	2252.670	3.93	0.062	0.064	2183.787	3.76	0.062	0.066
42	2253.207	3.40	0.062	0.064	2182.670	3.25	0.061	0.065
43	2253.738	3.00	0.062	0.064	2181.546	2.82	0.061	0.065
44	2254.261	2.51	0.062	0.064	2180.415	2.40	0.061	0.065
45	2254.513	2.14	0.061	0.064	2179.274	2.05	0.061	0.065

TABLE 1 continued.

46	2255.287	1.81	0.061	0.064	2178.134	1.74	0.061	0.065
47	2255.786	1.53	0.061	0.063	2176.970	1.47	0.061	0.065
48	2256.284	1.29	0.061	0.063	2175.826	1.23	0.061	0.065
49	2256.768	1.08	0.061	0.063	2174.653	1.03	0.061	0.065
50	2257.253	0.90	0.060	0.063	2173.490	0.86	0.061	0.064
51	2257.723	0.75	0.060	0.063	2172.310	0.72	0.061	0.064
52	2258.194	0.615	0.060	0.063	2171.129	0.59	0.061	0.064
53	2258.649	0.524	0.060	0.063	2169.935	0.486	0.061	0.064
54	2259.105	0.414	0.060	0.063	2168.741	0.396	0.061	0.064
55	2259.547	0.34	0.059	0.063	2167.533	0.325	0.061	0.063
56	2259.989	0.276	0.059	0.063	2166.325	0.260	0.060	0.063
57	2260.415	0.224	0.059	0.062	2165.101	0.22	0.060	0.063
58	2260.845	0.181	0.059	0.062	2163.884	0.17	0.060	0.063
59	2261.264	0.146	0.059	0.062	2162.682	0.135	0.060	0.063
60	2261.672	0.116	0.058	0.062	2161.416	0.11	0.060	0.063
61	2262.071	0.094	0.058	0.061	2160.173	0.09	0.059	0.062
62	2262.469	0.073	0.058	0.061	2158.922	0.069	0.059	0.062
63	2262.804	0.057	0.058	0.061	2157.662	0.051	0.059	0.062

where for $\Delta l = 0$, $m = J'' + 1$, $m = -J''$, and $m = 0$ for R-, P-, and Q-branches, respectively, and for $\Delta l = \pm 1$, $m = J'' + 1 \pm l''$, $m = -J'' \pm l''$, and $m = l''^2$ for R-, P-, and Q-branches, respectively. Table 2 presents the intensities S_v of the RV bands and the empirical parameters a_1 and a_2 of the F-factor for the indicated N_2O bands at the temperature $T = 296$ K.

The atlases of the ASL parameters of many gas components can be found in [20, 21], including the high-temperature atlas of the ASL parameters for NO given in [21].

TWO-BEAM SPECTROMETRY OF NITROGEN OXIDES

Detailed investigations of the absorption spectra of nitrogen oxides were performed on a two-beam spectral measuring installation with a two-beam multipass gas cell based on an IKS-24 spectrophotometer with limiting spectral resolution $\Delta = 0.5$ cm^{-1} [9]. Automation of recording and processing of results of measurements allowed absolute absorption spectra graduated in wave numbers to be obtained at 400–4000 cm^{-1}. The two-beam spectral installation allowed reference spectra of high accuracy to be obtained that were further used for parameterization of the spectral transmittance function (STF) and qualitative and quantitative analysis of ingredients of gas fuels and combustion products in power engineering and power technological units [2, 5, 18, 19]. Figure 4 shows the measured absorption spectra in $2\nu_1$, $\nu_1 + 2\nu_2$, and $\nu_1 + 3\nu_2 - \nu_2$ bands of pure N_2O for the indicated N_2O contents and P_{N_2O} pressures. Figures 5 and 6 show the NO_2 absorption spectra measured at 1200–1800 cm^{-1} and 400–100 cm^{-1}.

Nitrogen oxide (NO_2) formed oxide dimer N_2O_4. The reaction is reversible: $2NO_2 \leftrightarrow N_2O_4$. At a temperature of 262 K, the equilibrium was predominantly displaced toward the formation of N_2O_4. At temperatures exceeding 413 K, almost complete thermal dissociation of N_2O_4 was observed, when only NO_2 molecules were encountered in the medium. In the intermediate temperature interval $262 < T < 413$ K, the relationship between the volume concentrations $\rho(N_2O)$ and $\rho(N_2O_4)$ was determined by the temperature dependence of reaction rates of N_2O_4 formation and reverse reaction of N_2O_4 dissociation [22, 23].

The N_2O_4 molecule had 12 vibrational frequencies; in this connection, many combinational and overtone bands overlapped with the NO_2 bands were observed in the N_2O_4 spectra [16, 17]; in addition, N_2O_3 and N_2O_5 molecules formed as a result of the inverse dissociation reaction $2N_2O_4 \rightarrow N_2O_5 + N_2O_3$ [23] could be present. Table 3 gives the

TABLE 2. Measured Intensities S_ν, in $cm^{-2}\cdot atm^{-1}$ STP, and the Parameters a_1 and a_2 of the F-Factor of the $N_2^{14}O^{16}$ Bands at the Temperature $T = 296$ K

ν″–ν′	Band center, m^{-1}	S_ν, $cm^{-2}\cdot atm^{-1}$	a_1	a_2
$00^00 - 01^10$	588.767	32 ± 2	$5.3\cdot10^{-4}$	$3.9\cdot10^{-6}$
$01^10 - 02^00$	579.376	2.1 ± 0.2		
$01^10 - 02^20$	588.983	4.3 ± 0.3	$2.1\cdot10^{-3}$	$1.0\cdot10^{-6}$
$00^00 - 02^00$	1168.134	9.1 ± 0.7		
$01^10 - 03^10$	1160.291	15.6 ± 1.3		
$00^00 - 10^00$	1284.907	264 ± 20		
$01^10 - 11^10$	1280.520	13.13 ± 2		
$01^10 - 00^01$	1634.989	0.072 ± 0.005		
$00^00 - 03^10$	1749.058	0.063 ± 0.004		
$00^00 - 11^10$	1880.268	0.37 ± 0.02		
$01^10 - 12^20$	1886.018	0.046 ± 0.004		
$00^00 - 00^01$	2223.756	1484 ± 70	$3.2\cdot10^{-3}$	$3.8\cdot10^{-6}$
$01^10 - 01^11$	2209.523	196 ± 13	$3.9\cdot10^{-3}$	$4.0\cdot10^{-6}$
$05^10 - 01^10$	2309.109	0.14 ± 0.02		
$00^00 - 04^00$	2322.624	0.67 ± 0.06		
$00^00 - 12^00$	2461.998	8.62 ± 0.5	$2.8\cdot10^{-3}$	$4.1\cdot10^{-6}$
$01^10 - 13^10$	2457.446	1.36 ± 0.01	$3.4\cdot10^{-3}$	$3.2\cdot10^{-6}$
$00^00 - 20^00$	2563.341	35.41 ± 1	$2.3\cdot10^{-3}$	$5.9\cdot10^{-6}$
$01^10 - 21^10$	2577.090	3.99 ± 0.2	$3.7\cdot10^{-3}$	$2.3\cdot10^{-6}$
$00^00 - 01^11$	2798.290	2.21 ± 0.11		
$01^10 - 02^01$	2775.207	0.097 ± 0.01		
$01^10 - 02^21$	2784.370	0.26 ± 0.015		
$00^00 - 02^01$	3363.974	1.99 ± 0.12	$3.9\cdot10^{-4}$	$3.8\cdot10^{-5}$
$01^10 - 03^11$	3342.491	0.27 ± 0.02	$4.5\cdot10^{-4}$	$3.1\cdot10^{-6}$
$00^00 - 10^01$	3480.821	39.4 ± 2	$3.1\cdot10^{-4}$	0
$01^10 - 11^11$	3473.212	4.6 ± 0.07	0	$3.8\cdot10^{-5}$
$00^00 - 22^00$	3748.252	1.07 ± 0.04		
$01^10 - 23^10$	3747.031	0.14 ± 0.015		
$00^00 - 14^00$	3620.941	0.13 ± 0.02		
$00^00 - 30^00$	3836.373	1.74 ± 0.16		
$01^10 - 31^10$	3857.612	0.16 ± 0.02		
$00^00 - 11^11$	4061.979	0.023 ± 0.002		
$00^00 - 23^10$	4335.798	0.020 ± 0.002		
$00^00 - 00^02$	4417.379	1.44 ± 0.15	$6.7\cdot10^{-4}$	$1.7\cdot10^{-5}$
$01^10 - 01^12$	4388.928	0.15 ± 0.02	$5.6\cdot10^{-4}$	$1.5\cdot10^{-5}$
$00^00 - 12^01$	4630.164	0.15 ± 0.01		
$01^10 - 13^11$	4612.013	0.016 ± 0.02		
$00^00 - 20^01$	4730.828	1.12 ± 0.1		
$01^10 - 21^11$	4730.408	0.13 ± 0.02		
$00^00 - 01^12$	4977.695	0.0138		
$00^00 - 32^00$	5026.340	0.078 ± 0.007		
$00^00 - 40^00$	5105.650	0.072 ± 0.007		

frequencies of normal vibrations obtained by quantum mechanical calculations in the process of optimization of the geometric parameters and computation of normal vibration frequencies by the density functional method (DFT/B3LYP) with the 6-31G(d) basis set on the CSPEU (Kazan) computer cluster with application of the Gaussian 09. Revision A.01 package [15]. The strongest bands ν_4, ν_7, ν_9, and ν_{12} were identified in the spectra of ($NO_2 + N_2O_4$) mixtures shown in Figs. 5 and 6.

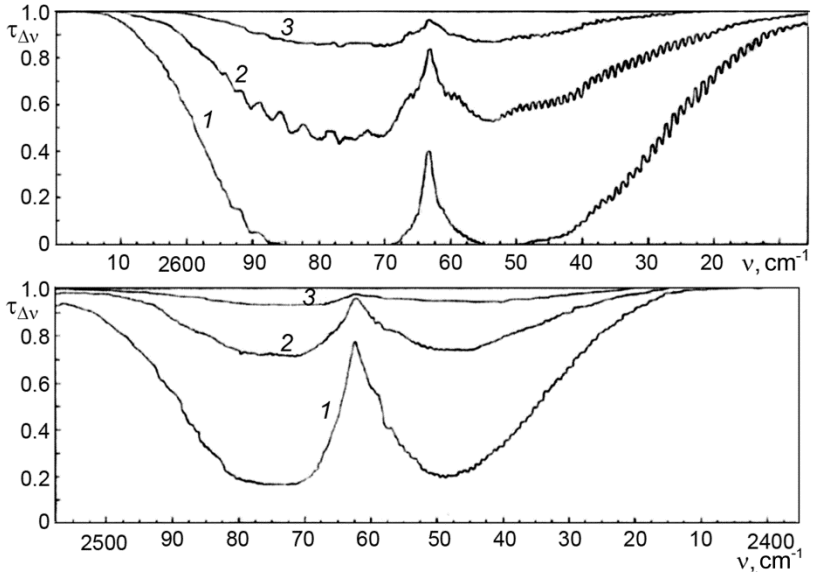

Fig. 4. Absorption spectra of nitrous oxide measured in $2\nu_1$, $\nu_1 + 2\nu_2$, $\nu_1 + 3\nu_2 - \nu_2$ bands for $w_{N_2O} = 10$ (curve *1*), 2.5 (curve *2*), and 0.625 atm·cm (curve *3*), $L = 10$ cm, $T = 300$ K, and $\Delta = 0.95$ cm^{-1}.

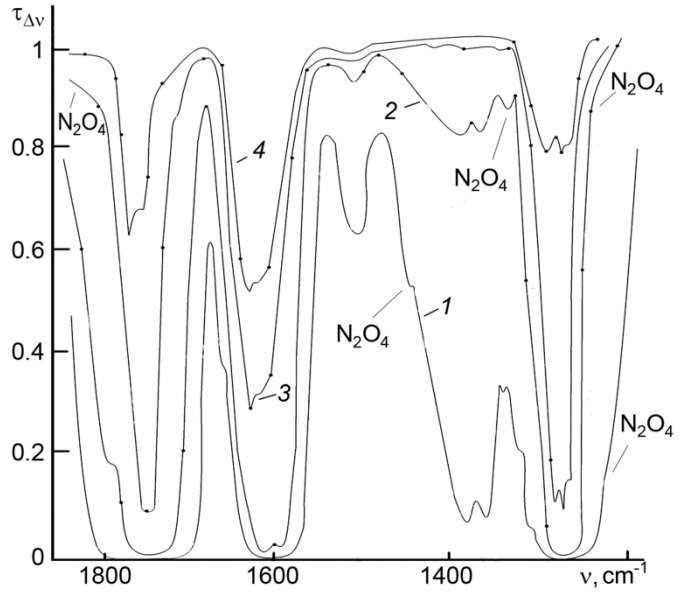

Fig. 5. Absorption spectra of ($NO_2 + N_2O_4$) mixtures at 1200–1800 cm^{-1}, total pressure $P = 0.641$ (curve *1*), 0.165 (curve *2*), 0.0493 (curve *3*), and 0.0118 atm (curve *4*), and $T = 296.5$ K.

Experimental investigations of the STF $\tau_{\Delta\nu}$ (Δ is the spectral resolution) of the ($NO_2 + N_2O_4$) mixtures allowed us to detect the presence of the PIA caused by the quadrupole moment induced in collisions of NO_2–NO_2 molecules. The most intense NO_2 PIA band was observed in the vicinity of 1750 cm^{-1}. Other NO_2 PIA bands were observed in the vicinity of wave numbers 510, 680, 1010, 1350, 1370, 1930, 2000, and 2580 cm^{-1}; they overlapped with the RV NO_2 and N_2O_4 bands.

TABLE 3. Normal Vibration Frequencies of the N_2O_4 Molecule

Vibration frequencies, cm^{-1}	95.2	229.2	229.2	433.2	500.3	681.1
Vibration frequencies, cm^{-1}	756.2	838.5	1330.6	1461.8	1829.0	1858.4

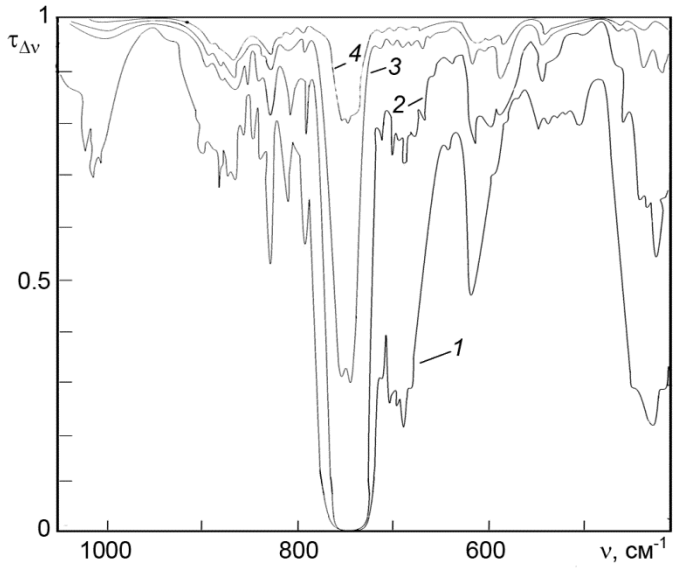

Fig. 6. Experimental absorption spectra of ($NO_2 + N_2O_4$) mixtures at 400–1000 cm^{-1}, total pressures $P = 0.641$ (curve *1*), 0.165 (curve *2*), 0.0493 (curve *3*), and 0.0118 atm (curve *4*), and $T = 296.5$ K.

The STF of the RV NO_2 and N_2O_4 and PIA NO_2 absorption bands were parameterized by the two-parameter equivalent mass method [8, 9], according to which for homogeneous paths

$$\left(\frac{1}{\ln\tau_{\Delta\nu}}\right)^2 = \left(\frac{1}{\ln}\right)^2 + \left(\frac{1}{\ln\tau''_{\Delta\nu}}\right)^2 + \frac{M}{\ln\tau'_{\Delta\nu}\ln\tau''_{\Delta\nu}}, \tag{8}$$

where

$$\tau'_\nu = \exp\left[-k_\nu w\right], \tag{9}$$

$$\tau''_\nu = \exp\left[-\beta_\nu w^{m_\nu} P_{\text{eff}}^{n_\nu}\right], \tag{10}$$

w is the content of the ingredient on the optical path L, P_{eff} is the effective pressure, $k\nu$, $\beta\nu$, $m\nu$, $n\nu$, and M are the STF parameters: $k\nu$ – in the approximation of weak absorption, $\beta\nu$, $m\nu$, and $n\nu$ – STF parameters in the approximation of strong absorption, and M – the parameter that defines the rate of STF transition from the approximation of weak absorption to the approximation of strong absorption. The parameter $M \in \{0,-1\}$ depends on the degree of overlap of the spectral lines of different gas components. The STF parameters $k\nu$ and $\beta\nu$ depend on the degree of overlap of the spectral lines for different gas components and on the temperature of the medium in which the emission propagates. The

TABLE 4. Parameters of the NO_2 Spectral Transmittance Function in the ν_3, ν_2, and $\nu_1 + \nu_3$ Fundamental Bands at $m = 0.84$, $n = 0.2$, and $M = -0.8$

ν, cm^{-1}	k_ν, $atm^{-1}\cdot cm^{-1}$	β_ν	ν, cm^{-1}	k_ν, $atm^{-1}\cdot cm^{-1}$	β_ν	ν, cm^{-1}	k_ν, $atm^{-1}\cdot cm^{-1}$	β_ν
620	0	0	890	0.075	0.06	1655	1.3	1.1
630	0.01	0.008	900	0.043	0.037	1660	0.26	0.21
640	0.019	0.015	910	0.017	0.014	1665	0	0
650	0.045	0.037	920	0	0	2340	0.018	0.015
660	0.12	0.1	1545	0	0	2845	0.036	0.03
670	0.17	0.14	1550	0.39	0.31	2850	0.055	0.045
680	0.26	0.21	1555	0.77	0.62	2855	0.092	0.074
690	0.27	0.23	1560	1.29	0.99	2860	0.2	0.16
700	0.31	0.26	1565	1.6	1.3	2865	0.28	0.22
710	0.37	0.31	1570	3.87	3.1	2870	0.41	0.33
720	0.47	0.39	1575	6.46	5.1	2875	0.61	0.5
730	0.55	0.45	1580	11.62	9.4	2890	0.77	0.62
740	0.47	0.39	1585	15.56	12.1	2895	0.93	0.75
750	0.4	0.32	1590	21.18	17.1	2900	0.98	0.79
760	0.5	0.4	1595	25.56	20.2	2905	0.98	0.79
770	0.57	0.45	1600	27.12	20.9	2910	0.93	0.75
780	0.52	0.42	1605	25.1	19.6	2915	1.1	0.9
790	0.42	0.34	1610	23.8	19.4	2920	1.19	0.98
800	0.35	0.28	1615	17.78	14.4	2925	0.92	0.74
810	0.3	0.24	1617	11.5	9.2	2930	0.5	0.4
820	0.27	0.21	1620	21.2	17.1	2935	0.29	0.23
830	0.26	0.2	1625	33.8	27.2	2940	0.12	0.093
840	0.21	0.17	1630	36.9	29.6	2945	0.039	0.032
850	0.18	0.14	1635	31	26.5	2950	0.01	0.008
860	0.15	0.12	1640	19.66	15.5	2955	0	0
870	0.12	0.1	1645	9.3	7.5			
880	0.107	0.09	1650	3.1	2.5			

inhomogeneities of the effective pressure and temperature in the medium along the optical path were taken into account in terms of the equivalent masses W' and W''in the approximations of weak and strong absorption; the computational algorithms for them in gaseous media with structurally inhomogeneous temperature, pressure, and chemical composition can be found in [8, 19]. The parameterization of the STF of nitrogen oxides was included in the electronic library of STF parameterization. As an example, Table 4 presents the STF parameters of the strongest fundamental NO_2 bands at the temperature $T = 300$ K. For the PIA, $m = n = 1$ and $M = -1$. From the experimental data, the values $(m + n) \in \{1.19; 2\}$, which confirms the occurrence of the PIA caused by the induced quadrupole moment in collisions of NO_2–NO_2 molecules in the NO_2 spectra.

HIGH-TEMPERATURE INVESTIGATIONS OF THE EMISSIVITY AND ABSORPTIVITY OF NITROGEN OXIDES

High-temperature investigations of the emissivity and absorptivity of nitrogen oxides were carried out on the measuring complexes described in [1, 3, 15, 16] and equipped with a MKhK-1 camera with electric heating at temperatures in the interval 300–900 K and on the flame measuring complexes at temperatures in the range 1200–

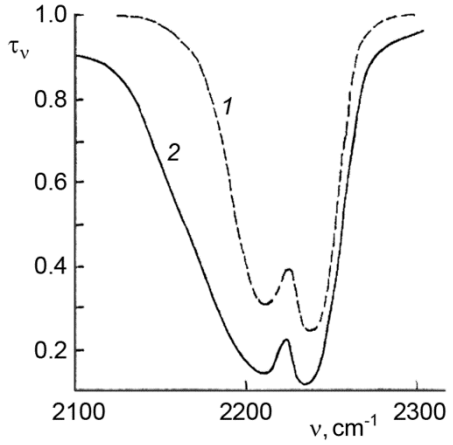

Fig. 7. N_2O absorption spectra in the vicinity of the 4.54 μm band at the temperatures T = 300 (curve *1*) and 2300 K (curve *2*), P = 1 atm, and w = 0.6 atm·cm STP.

2300 K with multi-row burners used to inject the desired oxide into the hydrogen-oxygen flame for combustion regimes with the oxygen excess coefficient $\alpha < 1$ in order to avoid the influence of oxidizing processes on the NO, N_2O, and NO_2 concentrations in the flame zone. At temperatures $T \geq 150$°C, N_2O_4 dissociated almost completely into NO_2, and no N_2O_4 bands were observed in the absorption spectra. An example of the N_2O absorption spectrum recorded in the vicinity of the fundamental band centered at 4.54 μm at temperatures of 300 and 2300 K is shown in Fig. 7. A comparison of the calculated NO STF and of the spectral absorption coefficients k_ν calculated using the high-temperature atlas of the ASL parameters [13] showed satisfactory agreement with the results of experimental investigations. In the UV and visible ranges of the electronic NO_2 emission spectrum, a strong influence of the nonequilibrium emissions in the zones of chemical reactions of burning of gaseous nitrogen-containing fuels was observed.

The data on the optical characteristics of nitrogen oxides obtained in this work have been used for solving problems of radiative heat exchange in high-temperature media [1–3], determination of ingredients of combustion products of organic fuels and anthropogenic atmospheric emissions of combustion products and prediction of the influence of strong anthropogenic and natural emissions on the climate of the Earth [5–9, 18, 19]. The application of atlases of the HITRAN 2010, 2013, and 2017 ASL parameters presented in [20, 21, 24] is promising for solving problems of emission transfer by the method of numerical integration of the fine structure of the spectrum.

REFERENCES

1. N. I. Moskalenko, S. O. Mirumyants, N. F. Loktev, and R. Sh. Misbahov, Equilibrium and Nonequilibrium Emission Processes: High-Temperature Media and Radiative Heat Exchange [in Russian], Publishing House of Kazan' State Power Engineering Universiy, Kazan' (2014).
2. N. I. Moskalenko, R. Sh. Misbahov, I. Z. Bagautdinov, *et al*., Russ. Aeronautics, **59**, No. 3, 419–425 (2016).
3. N. I. Moskalenko *et al*., in: Transfer of Nonequilibrium Emission in Flames and High-Temperature Media. Optoelectronics – Devises and Applications, Intechweb, ORG, Croatia (2011), pp: 469–526.
4. N. I. Moskalenko, M. S. Hamidullina, and Ya. S. Safiullina, Izv. Vyssh. Uchebn. Zaved. Probl. Energ., No. 3, 29–39 (2016).
5. N. I. Moskalenko, N. F. Loktev, *et al*., in: Engineering and Technology in the XXIst Century: Current State and Prospects for the Development. Book 4 [in Russian], CRNS-SIBPRINT Publishing House (2009), pp. 13–47, 48–87, 145–184.
6. N. I. Moskalenko *et al*., Izv. Vyssh. Uchebn. Zaved. Probl. Energ., Nos. 1–2, 23–33 (2012).

7. N. I. Moskalenko, Yu. A. Il'in, and G. V. Kayumova, Zh. Prikl. Spektrosk., **56**, No. 1, 377–381 (1992).
8. K. Ya. Kondrat'ev and N. I. Moskalenko, Green House Effect of the Atmosphere [in Russian], VINITI, Moscow (1984).
9. N. I. Moskalenko, S. N. Parzhin, and M. S. Hamidullina, Izv. Vyssh. Uchebn. Zaved., Probl. Energ., Nos. 5–6, 99–109 (2016).
10. N. I. Moskalenko *et al*., J. Appl. Spectrosc., **83**, No. No. 3, 449–453 (2016).
11. N. I. Moskalenko *et al*., J. Appl. Spectrosc., **83**, No. 5, 868–871 (2016).
12. N. I. Moskalenko, O. V. Zotov, Yu. A. Il'in, *et al*., Russ. Phys. J., **59**, No. 12, 2017–2024 (2017).
13. G. V. Kayumova, N. I. Moskalenko, and S. N. Parzhin, in: Abstracts of Reports Presented at the Vth All-Russian Symp. on Laser Radiation Propagation in the Atmosphere, Part 3 [in Russian], Tomsk (1979), pp. 182–186.
14. N. I. Moskalenko and O. V. Zotov, in: Abstracts of Reports Presented at the IVth Symp. on High and Ultrahigh Resolution Molecular Spectroscopy [in Russian], Novosibirsk (1978), pp. 97–102.
15. M. J. Frisch *et al*., Gaussian 09. Revision A1, Gaussian Inc., Pittsburgh (2017).
16. Y. Elyoussoufi, M. Herman, J. Lievin, and I. Kleiner, Spectrochim. Acta, Part A, **53** (6), 881–894 (1997).
17. O. K. Voitsekhovskaya, O. V. Egorov, and D. E. Kashirskii, Spectrochim. Acta, Part A, **165**, 47–53 (2016).
18. N. I. Moskalenko *et al*., Al'tern. Energ. Ekol., No. 2, 43–54 (2010).
19. N. I. Moskalenko, Ya. S. Safiullina, and M. S. Sadykov, Al't. Energ. Ekol., No. 2, 43–54 (2014).
20. L. S. Rothman *et al*., J. Quant. Spectrosc. Radiat. Transfer, **130**, 4–50 (2013).
21. L. S. Rothman *et al*., J. Quant. Spectrosc. Radiat. Transfer, **111**, 2139–2150 (2010).
22. V. I. Atroshenko and S. I. Kargin, Technology of Nitric Acid [in Russian], Goskhimizdat, Moscow (1962).
23. M. H. Freemantle, Chemistry in Action [Russian translation], Mir, Moscow (1998).
24. I. E. Gorden, L. S. Rothman, *et al*., J. Quant. Spectrosc. Radiat. Transfer, **203**, 3–69 (2017).